Predicting the initial rate of water absorption in clay bricks

Mariarosa Raimondo, Michele Dondi, Davide Gardini, Guia Guarini, Francesca Mazzanti

CNR-ISTEC, Institute of Science and Technology for Ceramics, via Granarolo, 64, 48018 Faenza (Italy)

Abstract. The effect of product characteristics and processing conditions on the initial rate of water absorption of fifteen clay bricks was investigated and the influence of porosimetric parameters (amount, size and tortuosity of pores) as well as of phase composition (amount of calcium-silicates and amorphous phase) was established. The suction behaviour of bricks, which may be brought back to the models of Gummerson et al. (1981) and Hoffman and Niesel (1988), was also evaluated on the basis of both the product microstructure and the liquid physical properties. According to the model of Beltran et al. (1988), which reveled to be sufficiently reliable, the values of the capillary coefficient K_s were calculated and their correlation with the experimental ones has been provided. For a given liquid and in the same experimental conditions, the results indicate that varying in a controlled way the product microstructure (i.e. decreasing the pore size, increasing the pore tortuosity and/or controlling the amorphous/new formed phases ratio) should allow to design materials having a most suitable behaviour.

Keywords: Traditional ceramics; Porosity; Microstructure-final; Capillary suction.

1. Introduction

In the structural design of masonry, the suction behaviour of its components - porous clay bricks and mortar - is one of the physical phenomena to be strictly controlled in order to optimize the mechanical performances and to prevent the occurrence, for example, of cracks, delaminations or soluble salts concentration leading to irreversible deterioration processes.[1-4] Focusing our attention on porous clay bricks as the main component of the masonry structure, their capacity of absorbing liquids and/or moisture, from both the immediate surrounding and the other building materials in association with them, can be referred as their "capillarity".[5, 6]

According to the latest standard,[7] clay bricks have to satisfy many different requirements in terms of thermal and acoustic properties, load-bearing capacity as well as ecological impact. The relationship between these properties and brick capillarity goes through the microstructural characteristics and, in particular, amount, size and shape of pores.[8] In fact, the capillarity phenomenon occurs as a consequence of the surface tension of a liquid in a capillary sistem, represented in this case by the narrow pores of the brick material. The quantification of the capillary suction can be realized by different test methods[9, 10] and can be determined quite easily without using expensive experimental techniques.

In the literature, many papers[1, 3, 4, 11, 12, 13] deal with the water uptake of different classes of porous materials, including paper, powders, rocks and soils, and a time dependent law of fluid absorption, taking the general form:

$$m = K_s \cdot t^{1/2} \tag{1}$$

seems to represent the basic kinetics of the suction process: the water absorbed by a porous solid per unit of surface area (*m*) increases as the square root of the elapsed time (*t*), with K_s being defined as the capillary coefficient.[14] This result is a generalization of the well-known Washburn equation, describing the horizontal movement of the meniscus in a capillary system, and it can be applied to the vertical movement in building materials in the early stages of capillary rise, negleting the contribution given by the weight of air columns. This is theoretically expected and is generally found, with some exceptions represented by materials presenting a markedly heterogeneous capillary structure.[15, 16]

Other mathematical functions describing the mass evolution of moisture and liquid rise, also in different experimental conditions, were empirically derived by Hoffman and Niesel, [17-19] and the simple relation (1) was replaced by an exponential one:

$$m = a \left[1 - \exp(-b t^{1/2})\right] \tag{2}$$

where *a* is the maximum moisture content, while *b* is a factor influencing the suction kinetics; multiplying *a* per *b*, the liquid absorption coefficient is obtained. This formula, which is able to replace the equation (1) for long-term processes, was statistically confirmed. [17]

Gummerson et al. [20] suggested, but did not prove, a certain dependence of the advance of meniscus into a cylindrical capillary on its radius; Lautridou and Ozouf [21], and Vos and Tammes [22], upon studying water suction in some calcareous rocks, commented that, for the same porosity, materials with a coarser pore size offer lesser resistance to suction than those with smaller pores.

Few trials to correlate the capillary uptake with physical properties of liquid and/or porous body are known; [23, 24] just one of the proposed models relates the so-called "capillarity" to the suction rate of liquids, their physical properties and the microstructure of porous bodies. [25-28] The equation (1) was further developed considering that the capillary coefficient K_s must depend on both properties of liquid (density, surface tension, contact angle formed by the meniscus with the capillary wall at the contact point) and of porous solid. According to this equation, the capillary coefficient is expressed by the formula:

$$K_s = \rho \left(\frac{\gamma}{\mu}\right)^{1/2} \frac{\varepsilon}{\lambda} r_0^{1/2} \left[\cos \vartheta / 2\right]^{1/2} \tag{3}$$

where ρ, γ and μ are, respectively, the density, the surface tension and the viscosity of the liquid, while ε represents the effective porosity (i.e. the open porosity actually accessible by the liquid), r_0 the median pore size and λ the pore tortuosity of the solid; θ is the liquid-brick contact angle. [25]

As at a given temperature the properties of the liquid are constant and can be grouped, together with the contact angle term, into a constant C, the equation (3) is reduced to:

$$K_s = C \cdot \frac{\varepsilon}{\lambda} \cdot r_0^{1/2} \tag{4}$$

while equation (1) can be written in the form:

$$m = \left[C \cdot \frac{\varepsilon}{\lambda} \cdot r_0^{1/2}\right] \cdot t^{1/2} \tag{5}$$

When the experimental results are represented graphically in the form of *m* versus $t^{1/2}$, a straight line with a slope K_s should be observed.

The aims of this work are i) giving a representative survey of the suction behaviour of the clay bricks; ii) appraising the applicability of the proposed models to predict the initial rate

of water absorption in clay bricks; iii) assessing the influence of the main microstructural and compositional parameters of clay bricks on the absorption process, considering the physical properties of water at the experimental temperature of 20°C as constant. The results pursued could permit an improvement in the evaluation of the effects of product and processing conditions on the capillary suction of porous bodies, thus representing an important starting point in the structural design of masonry components – porous brick elements and mortar – which are requested to present favourable performances in environmental conditions.

2. Materials and methods

Fifteen samples of clay bricks were collected in different brickworks, in order to represent the wide range of raw materials utilized by the Italian brick industry;[29] the sampling procedure and the manufacturing of clay brick elements have been described in detail elsewhere.[30]

All products were characterized by the determination of phase composition, open and total porosity, bulk density, pore size distribution and pore specific surface.

The phase composition was quantitatively determined by X-ray powder diffraction (Rigaku Miniflex, CuKα radiation) with the Reference Intensity Ratio method (Al_2O_3 as internal standard); the experimental error is within 5% relative.

Open porosity (OP) and bulk density (BD) were quantified by measuring dry weight, water-saturated weight and the weight suspended in water, according to ASTM C373.[31] Specific weight (SW) was measured by He pycnometry (Micromeritics MVP 1305) according to ASTM C329.[32] Total porosity (TP) was calculated by the equation: TP = (1-BD/SW) ·100.

The pore size distribution (in the 0.01 – 100 μm range) was determined by mercury intrusion porosimetry (Thermo Finnigan Pascal 140/240) with an experimental uncertainty of about 1% relative. In addition, the contact angle of mercury on the brick surface was experimentally determined (DataPhysics Instrument OCA 15); the resulting value of 166.4 ± 7.9°, obtained as the average of forty different measurements, indicates a lower wetting power of the mercury towards the product surfaces than expected. Owing to these circumstances, the pore size, obtained by mercury intrusion porosimetry assuming a fixed mercury contact angle of 141.3°,[33] was then corrected by a factor of 1.24 resulting by the insertion into the Washburn equation [34] of the experimental value of the mercury-brick contact angle. Porosimetric data are expressed as r_0 (median pore radius), amount of micropores (P50) having a diameter < 0.05 μm (i.e. < 50 nm) and amount of macropores (P3) having diameter > 3 μm.

The pore specific surface (SS) analyses were performed by nitrogen absorption (Micromeritics FlowSorb II 2300) following the B.E.T. single point method.[35]

The capillary absorption of samples was determined according to UNI 10859 [36] on circular disks (20.0 ± 0.1 cm diameter, thickness in the 1.5-2.0 cm range). Samples were preventively dried in an electric oven at 60 ± 2°C for 7 days and, after cooling, their weight (m_0) was measured. A basal face of each disk was put into direct contact with a 1 cm layer of paper, filled with distilled water at 20°C, in a closed vessel in order to reach saturation conditions. The water level was kept constant during the test. The mass of specimens (m_i) was recorded after 10, 20, 30 minutes and 1, 4, 6, 24, 48 and 72 hours. The liquid mass absorbed per surface unit area (m) was calculated by the formula:

$$m = (m_i - m_0)\ A^{-1} \tag{6}$$

where A is the area of the specimen in contact with the paper layer.

The capillary absorption of each sample was described plotting m versus the square root of the elapsed time, as schematically illustrated in figure 1A. The graph obtained presents a straight line, whose slope is the experimental capillary coefficient K_s, and a final stage characterized by an asymptotic trend.

In order to verify the equation (3), the following physical properties of water at 20°C were considered: density ρ = 0.998 g cm^{-3}; surface tension γ = 72.7 mN m^{-1}; viscosity μ = 1.0 mPa s. [24] The ε parameter was expressed, in the present work, as OP values. The water-brick contact angle was measured on the brick surface (DataPhysics Instrument OCA15) obtaining an average value of θ = 87± 3°; the capillary tortuosity factor λ, which is an empirical dimensionless parameter, was calculated as the ratio:

$$\lambda = \frac{r_0 \cdot SS \cdot BD}{2 \cdot OP} \qquad (7)$$

(for details see the appendix).

A statistical elaboration of data was performed by simple (linear binary correlation) and multivariate analysis techniques (factor analysis) using the StatSoft Statistica 6.0 software. Factor analysis was carried out on the main physical, compositional and microstructural variables extracting 4 factors according to the scree test for eigenvalues.[37]

3. Results and discussion

3.1 Physical properties

On the whole, samples show a great variability of their physical and microstructural parameters (table 1): total porosity is in the 19-43 %vol. range, mostly represented by open porosity (19-40 %vol). The median pore size r_0 is between 0.1 and 1.0 µm, while specific surface varies in the 0.6-2.4 m^2 g^{-1} range. An exception is represented by the sample SLA, which has the smallest pores (r_0 = 0.09 µm) developing a high specific surface (12.3 m^2 g^{-1}). The fraction of pores having dimensions under 50 nm (P50), generally below 6 %vol, is significant in the sample S (13.4 %vol), despite being the less porous material. On the other hand, the amount of the larger pores (P3) is maximum in samples RIN, MO and WPP.

The phase composition (figure 2) shows a certain variability of the amounts of both new formed and residual components. Samples are mainly made up of quartz (17-45%), with the amount of the residual K-feldspar and plagioclase up to 25 and 17%, respectively. Illite/mica is also present in most samples, with AT and SLA showing a content as high as 20%. The amorphous phase ranges from 6% (samples CAP and ZAP) to 45% (sample S), while, among the new formed phases, the total amount of pyroxene, wollastonite and melilite fluctuates between 2 and 46%.

3.2 Initial rate of water absorption

The suction behaviour of each sample is illustrated in figure 1B, where the liquid mass absorbed per unit area (m) is plotted versus the square root of the elapsed time (t) . Most samples reach the saturation condition after less than 3 hours, showing then an asymptotic trend involving very small variations of the liquid mass absorbed; nevertheless, the total amount of water absorbed varies from 0.05 g cm^{-2} of sample S to about 0.16-0.17 g cm^{-2} of samples AT, MO, WPP and WSN (table 2).

On the whole, samples seem to follow two main trends; most present an initial water uptake characterized by a steep slope (K_s values between 0.6 and 5.9 ·10^{-3} g cm^{-2}s$^{-1/2}$, figure 1B and table 2) that suddenly develops towards the asymptote, while samples S,

ILS and SLA exhibit a more gradual behaviour (K_s between 0.6 $\cdot 10^{-3}$ and 1.5 $\cdot 10^{-3}$ g cm^{-2}s$^{-1/2}$, table 2). These different trends can be brought back, respectively, to the models proposed by Gummerson and co-workers [14] or Hoffmann and Niesel [17]. In particular, the resistance (in terms of both m and K_s) offered by S, ILS and SLA to capillary suction has a first correspondence with their pore size and amount: the very low porosity and the significant percentage of micropores of sample S, as well as the smaller pores, when compared to the mean pore size of the other products, present in both ILS and SLA, confirm somehow the conclusions of the literature. [21, 22]

3.3 Capillary suction vs microstructural properties

In order to better understand the relationships between physical and microstructural characteristics of bricks and their liquid suction rate, an attempt was made to simply correlate K_s with the open and total porosity, median pore radius, amount of pores with a diameter under 50 nm or greater than 3 µm; this approach is based on the assumption that physical properties (i.e. density, viscosity, surface tension) of water are constant in the experimental conditions (atmospheric pressure and temperature of 20°C) so that liquid absorption depends only on the solid characteristics.

A positive correlation of both open (figure 3A) and total porosity (figure 3B) with K_s seems to exist though with a quite low statistical significance (r^2 = 0.524 and 0.347, respectively) mainly due to the sample MO, which presents a "capillary capacity" much higher than expected on the basis of its porosity. For this purpose, it is interesting to note that, looking at the correlation of the total amount of liquid absorbed m versus, for example, open porosity (figure 4), the behaviour of sample MO is lined up with the others suggesting, hence, a more complex dependence of K_s on the brick microstructure. In other words, if it is true that a less dense ceramic body is able to absorb a higher liquid amount for the same porosity, the influence of the other parameters characterizing the capillary structure is not obvious.

Concerning the relationships of K_s with the median pore size (r_0, figure 5A), the amount of pores smaller than 50 nm (P50, figure 5B) or greater than 3 µm (P3, figure 5C), the following conclusions can be drawn:

i) the suction kinetics does not seem dependent on the pore size since, for most samples, very different pore dimensions correspond to quite similar values of K_s; moreover, the correlation factor (r^2 = 0.015) is heavily influenced by samples S and MO, whose rather small difference of pore size is translated into a great difference in terms of absorption coefficient;

ii) the correlation of K_s with P50 gives rise to a cloudy distribution of data (r^2 = 0.269) also because, among the samples, there are not big differences in the relative amount of micropores; at all events, the behaviour of sample S, having P50 as high as 13.4%, suggests that the presence of such micropores could represent an effective restriction to the liquid uptake;

iii) on the other hand, when K_s is plotted against P3, the correlation has a quite low statistical significance (r^2 = 0.034), so that the statement that larger pores should be the most involved in the suction phenomenon [25] was proved to be not completely reliable.

Owing to these results and making provision for a more complex dependence of the liquid uptake process on the solid microstructure and the solid-liquid interactions, the effectiveness of equation (3) in predicting K_s values was investigated.

3.4 Predicting the capillary coefficient K_s

The reliability of the model proposed by Beltràn and co-workers [25-28] was checked introducing into the equation (3) the physical data of water (density, surface tension and

viscosity, as calculated at 20°C) and, for each sample, the experimental values of open porosity, median pore size, water-brick contact angle (θ = 87°) and tortuosity factor as calculated in the present work.

The predicted K_s values obtained range from 3.4 $\cdot 10^{-3}$ (g cm^{-2}s$^{-1/2}$) of sample SLA to 25.1 $\cdot 10^{-3}$ (g cm^{-2}s$^{-1/2}$) of sample MO (K_s^*, table 2) and their correlation with the experimental ones being illustrated in figure 6; fitting the results by linear regression, the straight line going through the origin provides the following relationship (r^2 = 0.692): the value of the capillary coefficient K_s^* predicted on the basis of equation (3) has to be multiplied by 0.212 to obtain the experimental one so that the real suction kinetics of all samples is proved to be lower than expected on the basis of Beltran's model.

Focusing our attention on these aspects, both predicted and experimental values of the capillary coefficient were plotted as function of the term OP/λ $(r_0)^{1/2}$ (figure 7); the linear fitting provides straight lines having, respectively, the form:

$$K_s = 2.915 \frac{OP}{\lambda} (r_o)^{1/2} \qquad (r^2 = 0.692) \tag{8}$$

and

$$K_s^* = 13.760 \frac{OP}{\lambda} (r_o)^{1/2} \qquad (r^2 = 1) \tag{9}.$$

As expected, the ratio between the slope values (2.915/13.760 = 0.212) coincides with the slope of the straight line fitting the experimental/predicted K_s relationship. Moreover, the slope value of equation (8) must correspond to the term: $\rho(\frac{\gamma}{\mu})^{1/2}[\cos \vartheta / 2]^{1/2}$ which, considering constant the physical data of water at 20°C, provides the value of the water-brick contact angle fitting the experimental results: θ = 89°; this value is very similar to the average value (θ = 87°) utilized in the present work, which has been experimentally determined.

Looking back at equation (8) and figure 7, it is reliable to conclude that, besides some exceptions, the Beltràn's model is sufficiently satisfied: for the same value of open porosity, decreasing the pore size and/or increasing the pore tortuosity means to limit the suction rate and, hence, the capacity of clay bricks of absorbing moisture. At any event, this also means that, varying in a controlled way the product OP/λ $(r_0)^{1/2}$, it could be possible to design clay bricks having a more suitable suction behaviour and, at least, to bound the structural deterioration of masonry optimizing the performance of its components.

3.5 Capillary suction vs phase composition

Since in the literature the influence on the suction kinetics of both amount of $CaCO_3$ in the starting mixtures and firing temperature was also investigated,[27] we tried to assess the possible role played by the brick phase composition, particularly Ca-silicates and amorphous content, on K_s.

From a microstructural point of view, the decomposition of $CaCO_3$ during firing, with the formation of Ca-silicates by reaction with the clay mineral and release of CO_2, promotes a greater amount of porosity; theoretically, this circumstance it is expected to cause higher values of K_s and, in our case, it is somehow confirmed (figure 8A).

On the other hand, the amount of amorphous phase originating from an incomplete rearrangement of clay minerals, together with the low sintering degree achieved at the typical brick firing temperature (900-1000°C), involve the presence of a smaller porosity, which, in turn, seems to be a restriction to the liquid suction phenomenon (figure 8B).

In order to better evaluate both these latter relationships and the previous ones, expecially when very low correlation factors came out, a statistical treatment of data was undertaken through the extraction of the principal components; this procedure allows to classify all the investigated parameters into different groups and to reduce the number of significant variables.[37] In the statistical approach, the amount of Ca-silicates and amorphous phase, other than K_s, were also considered as variables in addition to the microstructural ones (OP, TP, r_0, P50, P3, SS, λ). The analysis of the main components extracted three significant factors, accounting for 83% of the total variance (table 3). Factor 1 explains most of the variance of some physical (OP, TP) and microstructural (P50) parameters and confirms the role of the composition (Ca-silicates and amorphous phase) while factors 2 and 3 account, respectively, for the variance of pore dimension (in terms of both median radius and amount of micropores) and specific surface. The positive or negative influence of each variables on K_s clearly stands out when the factorial weights are plotted grafically (figure 9). A higher porosity, in terms of both open and total values, makes the liquid uptake faster. The restrictive role played by the amount of micropores and the amorphous phase on the water suction rate is also underlined by the statistical procedure, as well as the opposite role played by the new formed Ca-silicates.

4. Conclusions

The suction behaviour of clay bricks, in terms of liquid mass adsorbed as function of time, follows two main trends which can be brought back, respectively, to the models of Gummerson et al. [14] and Hoffmann & Niesel [17-18]: the amount of absorbed water increases as the square root of the time, with a starting straight line, whose slope is represented by the capillary coefficient K_s, and a final asymptotic trend. These models, however, do not provide any information about the liquid-solid interactions, so that no prediction of the material behaviour in working conditions can be done.

Considering the capillarity phenomenon, the suction capacity of bricks is expected to depend on their microstructural characteristics, in particular, amount, size and shape of pores. Besides some exceptions, the linear relationships between the capillary coefficient K_s and these microstructural variables substantially confirm the role played by open porosity in increasing the absorption capacities of clay bricks, while the influence of pore characteristics (dimension, tortuosity or internal specific surface) on the suction kinetics does not clearly stand out.

Making provision for a higher complexity of the liquid uptake process, the values of the capillary coefficient K_s were also calculated on the basis of Beltrán and co-workers [25], whose effectiveness in predicting K_s values proved to be quite good. This means that, varying in a controlled way the term *OP/λ* $(r_0)^{1/2}$, it is possible to design materials having a predictable suction behaviour, hence to bound the damages in terms of structural deterioration.

The capillary coefficient K_s, together with the microstructural variables and phase composition, finally underwent a statistical procedure that confirmed the influence of porosity, as well as of a coarser pore dimension (in terms of both radius and percentage of pores greater than 3 μm) in increasing the liquid adsorbing rate with the highest statistical significance. In addition, the sintering pattern of products, leading to a different amorphous/crystalline phases ratio, proved to be relevant on the definition of the most suitable microstructure: the higher porosity, promoted by the complete $CaCO_3$ decomposition, and the smaller pore size, connected with the low sintering degree of clay bricks, work in the opposite way.

Appendix

The pore tortuosity λ is a non-dimensional parameter

$$\lambda = \frac{l}{L} \tag{10}$$

defined with reference to a cylindrical brick of area A and thickness L with a number N' (g^{-1}) of open pores per unit mass; these capillary pores have length l and radius r_0 (figure 10).

Straight and regularly shaped pores have a shorter length l in respect of tortuous pores of the same radius, reflecting in smaller values of specific surface area SS ($m^2\ g^{-1}$), since:

$$SS = N'\ 2\ \pi\ r_0 l \tag{11}$$

As the surface porosity ε (adim.) can be calculated by:

$$\varepsilon = \frac{N' \cdot \pi \cdot r_0^{\ 2}}{A'} \tag{12}$$

where A' ($cm^2\ g^{-1}$) is the total surface area per unit mass, the number of pores can be obtained by:

$$N' = \frac{\varepsilon \cdot A'}{\pi \cdot r_0^{\ 2}} \tag{13}$$

and the specific surface area can be expressed, replacing eq. (13) into eq. (11):

$$SS = \frac{\varepsilon \cdot A'}{\pi \cdot r_0^{\ 2}}\ 2\ \pi\ r_0 l = \frac{2\varepsilon \cdot A' \cdot l}{r_0} \tag{14}$$

The pore length l can be extracted as:

$$l = \frac{SS \cdot r_0}{2\varepsilon \cdot A'} \tag{15}$$

so that substituting eq. (15) into eq. (10):

$$\lambda = \frac{l}{L} = \frac{SS \cdot r_0}{2\varepsilon \cdot A' \cdot L} \tag{16}$$

Knowing that the surface area can be expressed as:

$$A' = \frac{A}{m} = \frac{V}{m \cdot L} = \frac{1}{BD \cdot L} \tag{17}$$

where m is the mass, V the volume and BD the bulk density, i.e. the m/V ratio, replacing eq. (17) into eq. (16) the pore tortuosity is calculated as:

$$\lambda = \frac{SS \cdot r_0 \cdot BD \cdot L}{2\varepsilon \cdot L} = \frac{SS \cdot r_0 \cdot BD}{2\varepsilon} \tag{18}$$

References

1. Anand K. B., Vasudevan V. and Ramamurthy K., *Water permeability of alternative masonry systems*. Build. Environ. 2003, **38**, 947-957.
2. Künzel H. M. and Kiessl K., *Calculation of heat and moisture transfer in exposed building components.* Int. J. Heat Mass Transfer, 1997, **40** (1), 159-167.
2. Wilson M. A., Hoff W. D. and Hall C., *Water movement in porous building materials-XIII. Absorption into a two layer composite*. Build. Environ., 1995, **30** (2), 209-219.
4. Wilson M. A., Hoff W. D. and Hall C., *Water movement in porous building materials-XIV. Absorption into a two layer composite ($S_A<S_B$)*. Build. Environ.,1995, **30** (2), 221-227.
5. Roβbach M., *Capillary suction property of bricks*. Ziegelindustrie Annual, 1998, 90-101.
6. Ridgway C. J., Gane P. A. C. and J. Schoelkopf, *Achieving rapid absorption and extensive liquid uptake capacity in porous structures by decoupling capillarity and permeability: nanoporous modified calcium carbonate.* Transp. Porous Med., 2006, **63**, 239-259.
7. UNI EN 771-1. Specification for masonry unit. Part. 1: Clay masonry units. 2003.
8. Raimondo M., Dondi M., Mazzanti F., Stefanizzi P. and Bondi P., *Equilibrium moisture content of clay bricks: the influence of the porous structure.* Build. Environ., 2007, **42**, 926-932.
9. Niesel K., *Quelques aspects expérimentaux de l'etude du transfert d'humidité en maçonnerie*. Silic. Ind., 1989, **3-4**, 47-54.

10. Drchalová J. and Černý R., *A simple gravimetric method for determining the moisture diffusivity of building materials*. Constr. Build. Mater., 2003, **17**, 223-228.

11. Hall M. and Djerbib Y., *Moisture ingress in rammed earth: Part 1-The effect of soil particle-size distribution on the rate of capillary suction.* Constr. Build. Mater., 2004, **18**, 269-280.

12. Smiles D. E., *Water flow in filter paper and capillary suction time*. Chem. Eng. Sc., 1998, **53** (12), 2211-2218.

13. Pasculli A. and Sciarra N., *A numerical one-dimensional modelling of water transport through a porous material under saturated and unsaturated condition: parametric studies*. Mem. Soc. Geol. It., 2001, **56**, 367-374.

14. Gummerson R. J., Hall C. and Hoff W. D., *The suction rate and the sorptivity of bricks*. Brit. Ceram. Trans. J., 1981, **80**, 150-152.

15. Küntz M. and Lavallée P., *Experimental evidence and theoretical analysis of anomalous diffusion during water infiltration in porous building materials.* J. Phys. D: Appl. Phys., 2001, **34**, 2547-2554.

16. Lockington D. A. and Parlange J. Y., *Anomalous water absorption in porous materials.* J. Phys. D: Appl. Phys., 2003, **36**, 760-767.

17. Hoffmann D. and Niesel K., *Quantifying capillary rise in columns of porous material*. Am. Ceram. Soc. Bull., 1988, **67** (8), 1418.

18. Hoffmann D., Niesel K. and Wagner A., *Capillary rise and the subsequent evaporation process measured on columns of porous material.* Am. Ceram. Soc. Bull., 1990, **69** (3), 392-396.

19. Hoffmann D., Niesel K. and Plagge R.*, Water retention and conductivity of porous media.* Am. Ceram. Soc. Bull., 1995, **74**, (11), 48-50.

20. Gummerson R. J., Hall C. and Hoff W., *Water transport in porous building materials – II. Hydraulic suction and sorptivity of bricks and other masonry materials,* Build. Environ., 1980, **15**, 101.

21. J. P. Lautridou, J. C. Ozouf, *Relations entre la gelivité et les propriétés (porosité, ascensión capillaire) des roches calcaires.* Colloque int. UNESCO-RILEM. Alteration et protection des monuments en pierre, Paris 5 June, 1978.

22. Vos B. H. & Tammes E., *Moisture and moisture transfer in porous materials*. *Report no BI-69-96*, Institute TNO for building materials and building structures, Delft, Holland, 1969.

23. Hall C., Hoff W. D. and Prout W., *Sorptivity-porosity relations in clay brick ceramic,* Am. Ceram. Soc. Bull., 1992, **71** (7), 1112-1116.

24. Freyburg S. and Schwarz A., *Influence of the clay type on the pore structure of structural ceramics.* J. Eur. Ceram. Soc., 2006, **27**, 1727-1733.

25. Beltrán V., Escardino A., Feliu C. and Rodrigo M. D., *Liquid suction by porous ceramic materials.* Br. Ceram. Trans. J., 1988, **87**, 64-69.

26. Beltrán V., Barba A., Rodrigo M. D. and Escardino A., *Liquid suction by porous ceramic materials: 2. – Influence of pressing conditions*. Br. Ceram. Trans. J., 1989, **88**, 219-222.

27. Beltrán V., Barba A., Jarque J. C. and Escardino A., *Liquid suction by porous ceramic materials: 3. – Influence of the nature of the composition and the preparation method of the pressing powder.* Br. Ceram. Trans. J., 1991, **90**, 77-80.

28. Escardino A., Beltrán V., Barba A. and Sánchez E., *Liquid suction by porous ceramic materials: 4. – Influence of firing conditions.* Br. Ceram. Trans. J., 1999, **98** (5), 225-229.

29. Dondi M., Ercolani, G., Fabbri B., Guarini, G., Marsigli M., Mingazzini C., *Major deposits of brick clays in italy. Part 1: Geology and composition*. Tile & Brick Int., 1999, **15** (4), 230-237. *Part 2: Technological properties and uses.* Tile & Brick Int., 1999, **15** (5), 360-370.

30. Dondi M., Principi P., Raimondo M. and Zanarini G., *The thermal conductivity of bricks produced with Italian clays.* L'Ind. dei Later., 2000, **65**, 309-320.

31. ASTM C 373, *Water absorption, bulk density, apparent porosity, and apparent specific gravity of fired whiteware products*. American Society for Testing and Materials, 1994.

32. ASTM C 329, *Specific gravity of fired ceramic whiteware materials.* American Society for Testing and Materials, 1994.

33. Winslow, N. M. and Shapiro, J. J., *An instrument for the measurement of pore- sized distribution by mercury penetration*: A. S. T. M. Bull., 1959, **236**, 39-54.

34. Washburn E. W., *Note on a method of determining the distribution of pore sizes in a porous material*. Proc. Nat. Acad. Sci., 1921, **7**, 115-116.

35. ASTM C 1069, *Specific surface area of alumina or quartz by nitrogen adsorption.* American Society for Testing and Materials, 1997.

36. UNI 10859, *Cultural heritage – Natural and artificial stones – Determination of water absorption by capillarity*. UNI, Ente Italiano di Unificazione, 2000.

37. Cooley W. W. and Lohnes P. R., *Multivariate data analysis*. Wiley, New York, 1971.

Table 1. Open (OP) and total (TP) porosity, bulk density (BD), median pore radius (r_0), specific surface (SS), amount of pores having a diameter smaller than 0.05 μm (P50) and greater than 3 μm (P3), pore tortuosity (λ) and thickness of clay bricks.

Samples	OP (%vol)	TP (%vol)	BD (g cm^{-3})	r_0 (μm)	SS (m^2 g^{-1})	P50 (%vol)	P3 (%vol)	λ (adim.)	Thickness (cm)
AT	39.0	42.6	1.605	0.48	2.40	2.7	1.2	2.4	1.83
CA	33.3	34.9	1.763	0.66	2.00	0.9	1.1	3.6	1.95
CAN	36.0	39.3	1.696	0.61	2.02	0.8	0.8	2.9	1.49
CAP	36.7	38.4	1.684	0.61	1.87	0.1	0.6	2.6	1.65
F	24.4	27.3	1.870	0.42	1.00	0.6	0.5	1.6	1.55
ILS	27.7	37.5	1.716	0.38	1.90	1.5	1.1	2.2	1.84
MO	36.3	36.5	1.766	0.43	1.20	0.7	4.5	1.3	2.02
RIN	33.3	36.2	1.712	0.99	2.11	4.2	4.8	5.4	1.47
RIP	32.7	34.0	1.715	1.00	1.47	5.8	4.2	3.9	1.63
S	18.8	18.8	2.121	0.61	0.60	13.4	1.6	2.1	1.62
SLA	28.9	28.9	1.896	0.09	12.30	0.8	1.2	3.5	2.02
WPP	36.5	38.6	1.657	1.00	1.61	3.1	6.1	3.7	2.15
WSN	35.2	38.1	1.673	0.84	1.40	0.8	2.7	2.8	2.07
ZAN	38.5	41.0	1.632	0.54	2.30	0.8	1.2	2.6	1.62
ZAP	38.4	41.4	1.627	0.56	2.36	0.6	2.2	2.8	1.58

Table 2. Total amount of absorbed water (m), experimental (K_s) and predicted (K_s*) values of capillary coefficient.

Samples	m (g cm^{-2})	$K_s \cdot 10^3$ (g cm^{-2}s$^{-1/2}$)	$K_s^* \cdot 10^3$ (g cm^{-2}s$^{-1/2}$)
AT	0.164	3.1	15.4
CA	0.144	3.3	10.4
CAN	0.124	2.8	13.2
CAP	0.139	3.0	15.2
F	0.095	1.9	13.3
ILS	0.125	1.5	10.8
MO	0.165	5.9	25.1
RIN	0.100	2.2	8.4
RIP	0.108	2.3	11.7
S	0.052	0.6	9.7
SLA	0.138	1.5	3.4
WPP	0.165	3.4	13.4
WSN	0.155	3.5	15.7
ZAN	0.121	3.1	15.2
ZAP	0.139	3.1	13.9

Table 3. Results of the extraction of the main components: factorial weights.

Variable	Factorial weights Extraction of the main components		
	Factor 1	Factor 2	Factor 3
Open porosity	0.9100	0.0635	0.2994
Pore tortuosity	-0.0024	0.6808	0.6423
Total porosity	0.9386	-0.0203	0.1983
Amount of pores > 3μm	0.1935	0.7975	0.0725
Capillary coefficient K_s	0.7552	0.0104	-0.0447
Median pore size	0.2504	0.9186	-0.1348
Specific surface	-0.3263	-0.3621	-0.8371
Amount of pores < 0.05 μm	-0.6748	0.5008	-0.3511
Amorphous phase	-0.8577	0.0626	0.0132
Ca-silicates*	0.7752	-0.2009	-0.4592
Explained variance	42.78	23.75	16.02

* Sum of plagiocalse + pyroxene + melilite + wollastonite
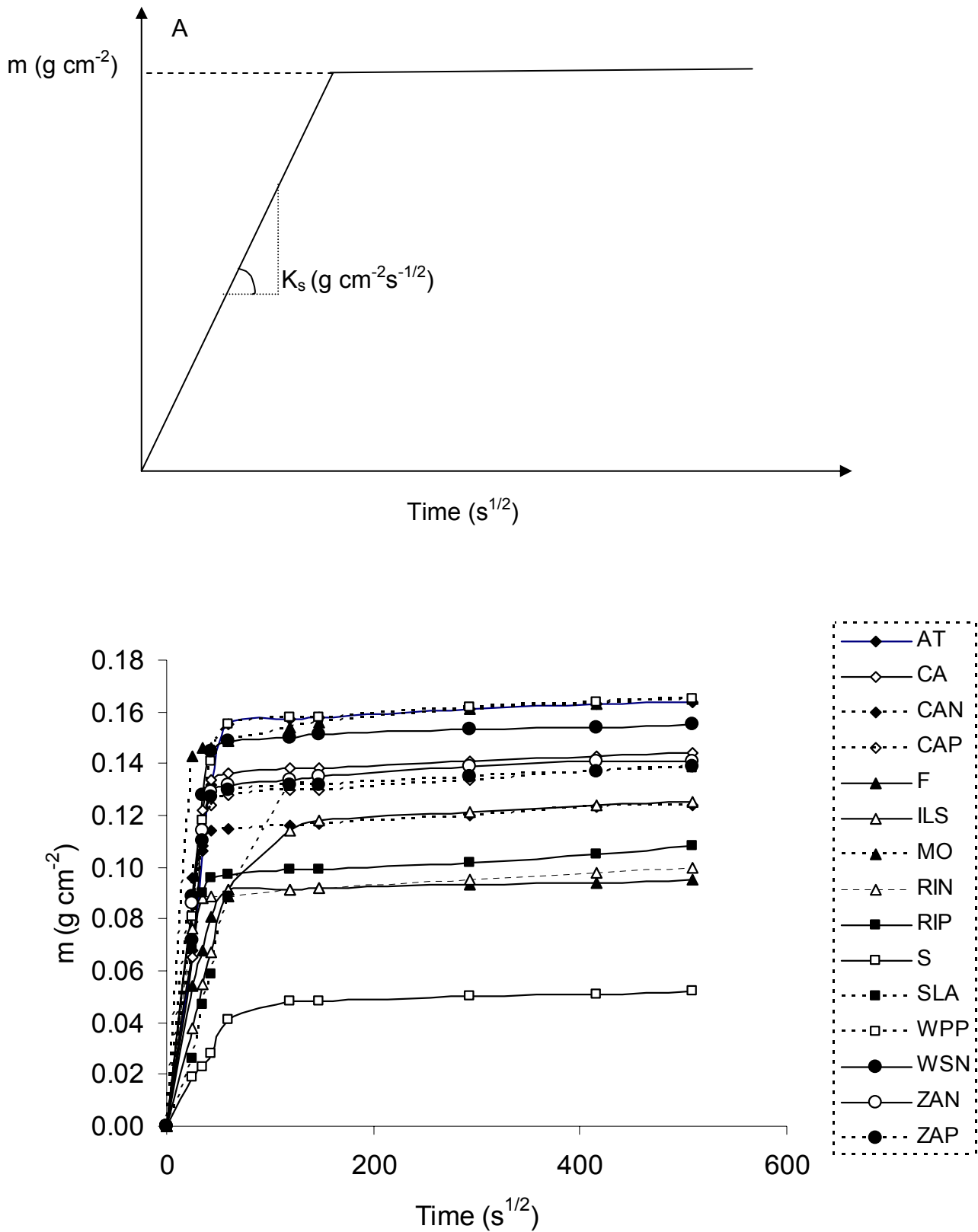
Figure 1. (A) Calculation of total amount of water absorbed *m* (g cm^{-2}) and of capillary coefficient K_s (g cm^{-2}s$^{-1/2}$) and (B) suction behaviour of clay bricks.
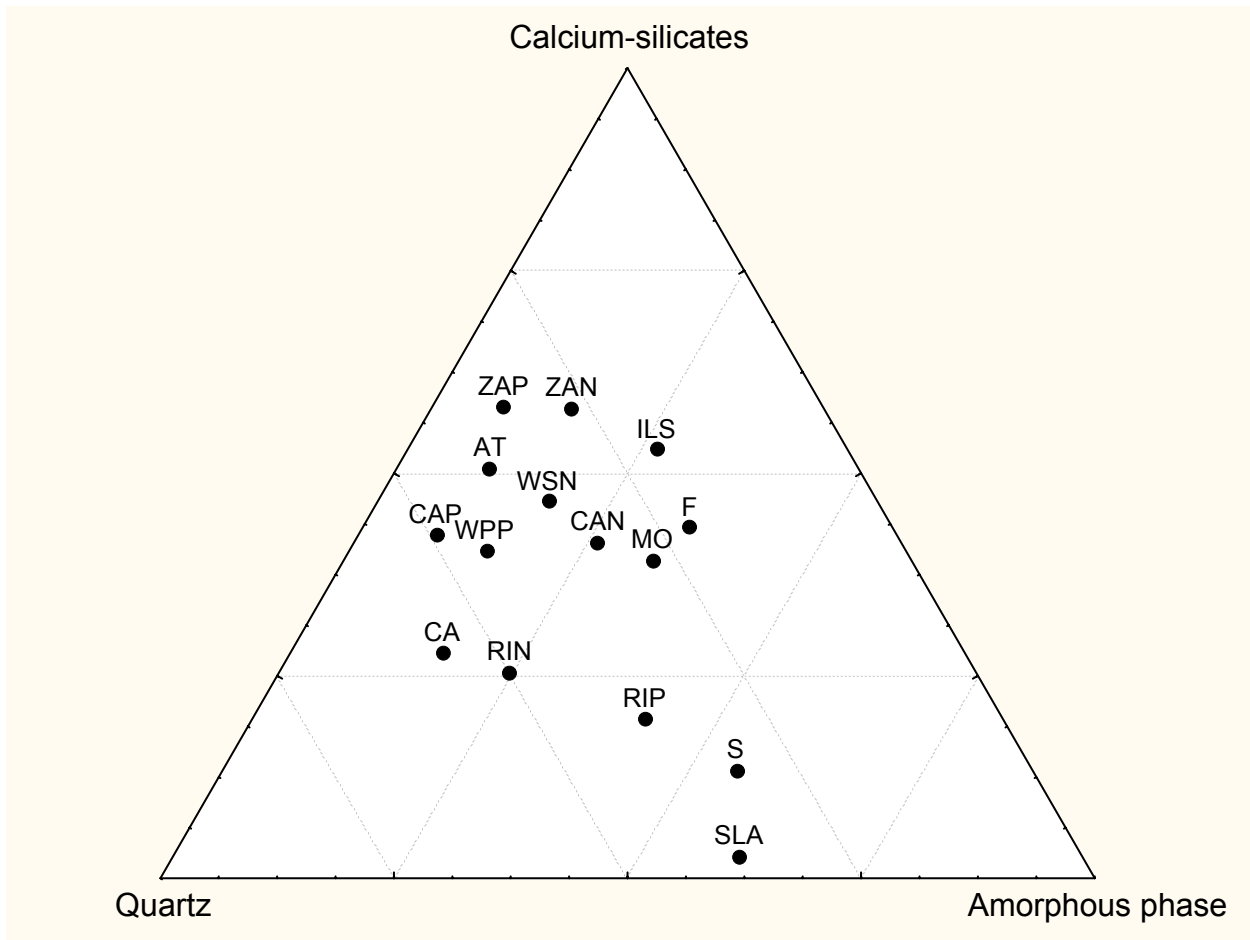
Figure 2. Phase composition of clay bricks. Calcium-silicate: plagioclase + clinopyroxene + melilite + wollastonite.
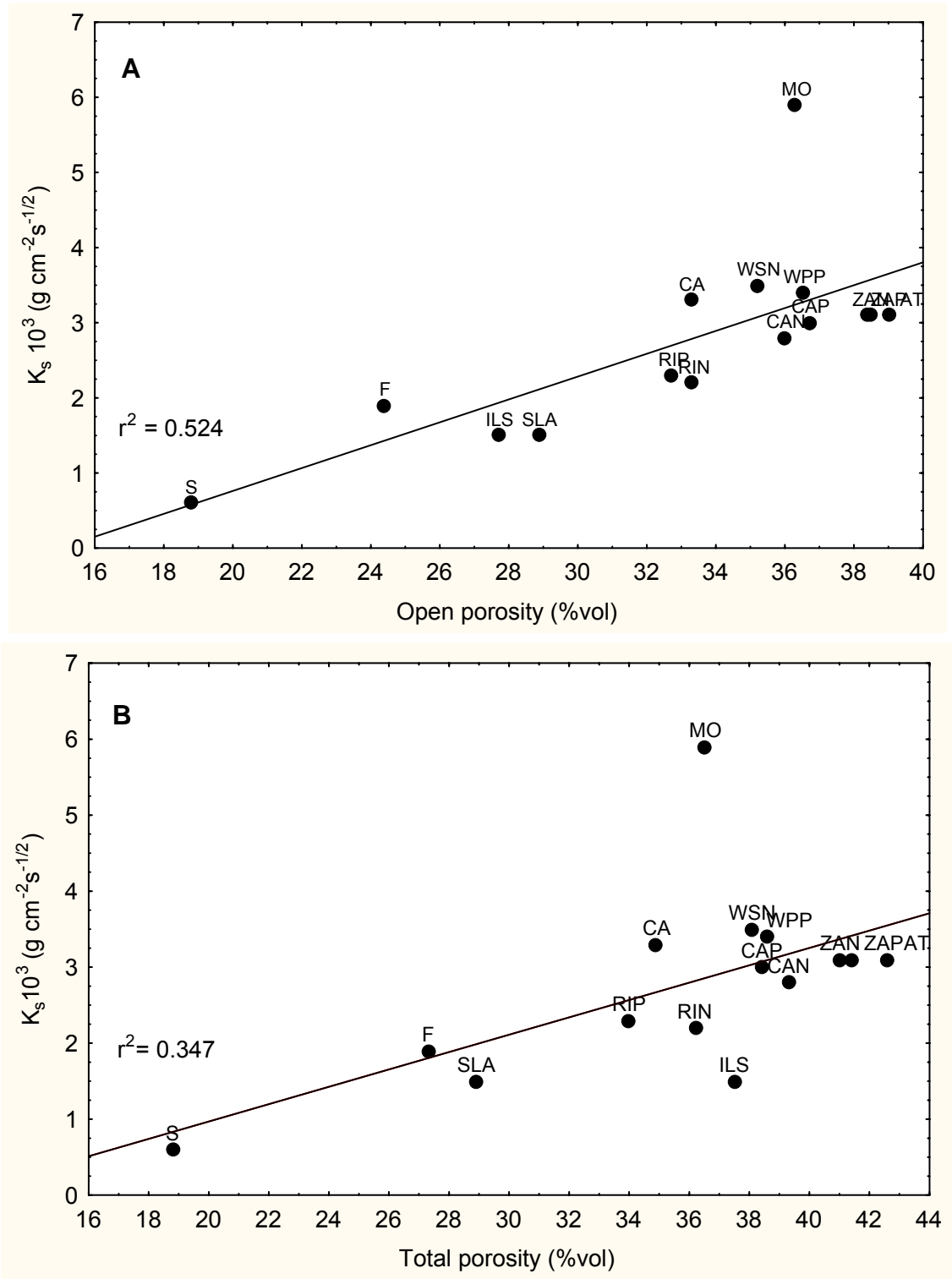
Figure 3. Experimental capillary coefficient K_s vs. (A) open porosity and (B) total porosity of clay bricks.
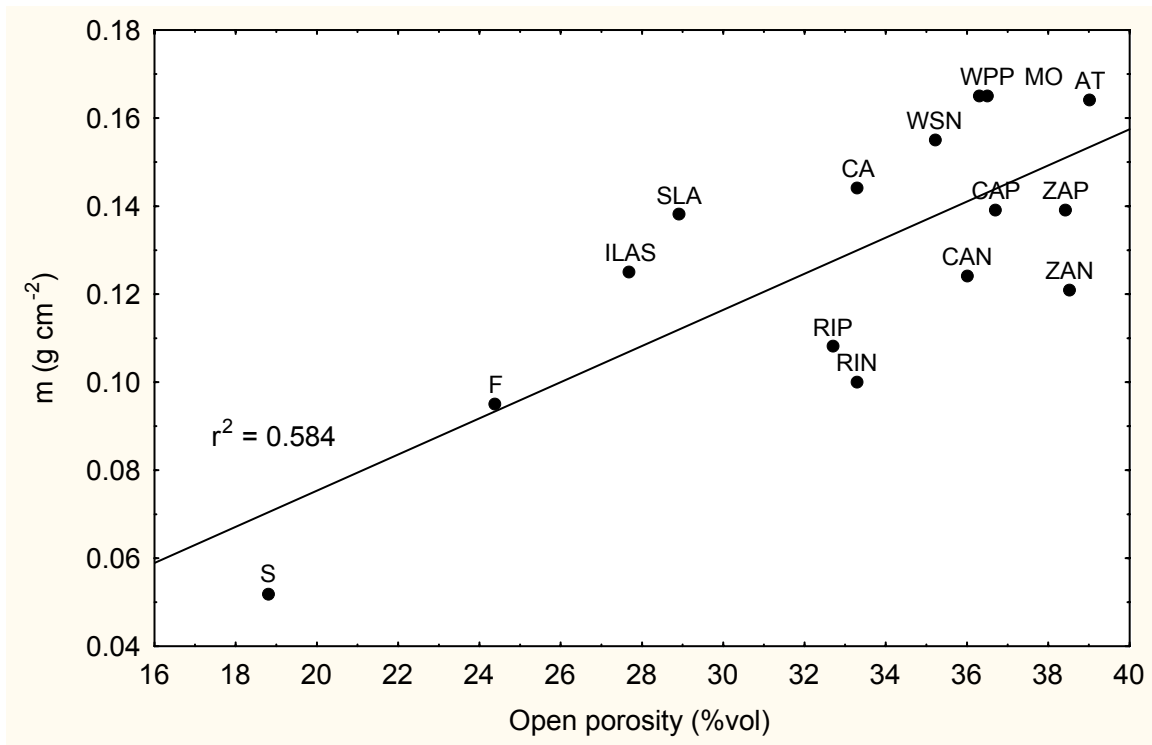
Figure 4. Amount of water absorbed *m* (g cm^{-2}) vs. open porosity of clay bricks.
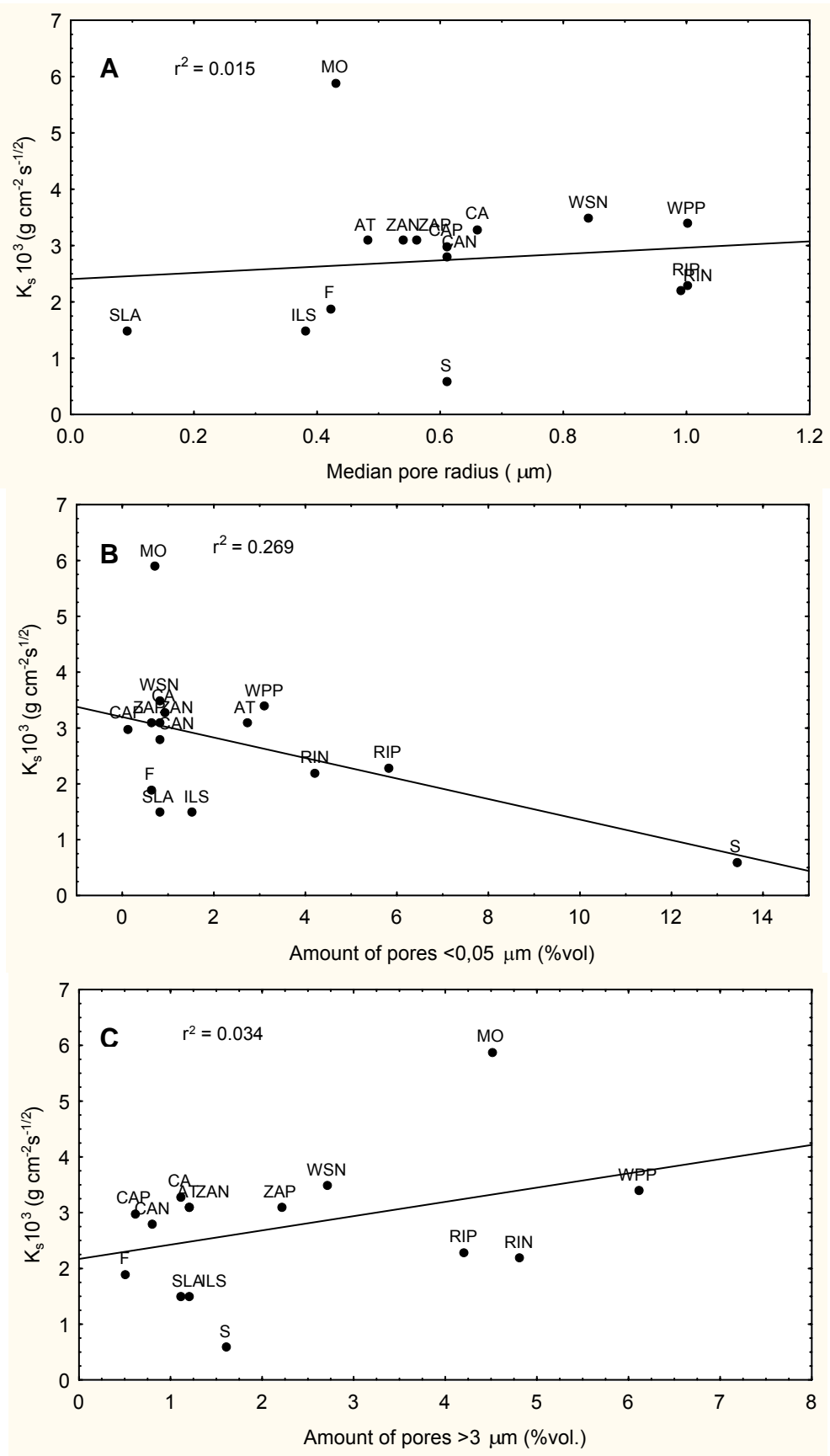
Figure 5. Experimental capillary coefficient K_s vs. (A) median pore size, (B) amount of pores <0.05 μm and (C) amount of pores >3 μm.
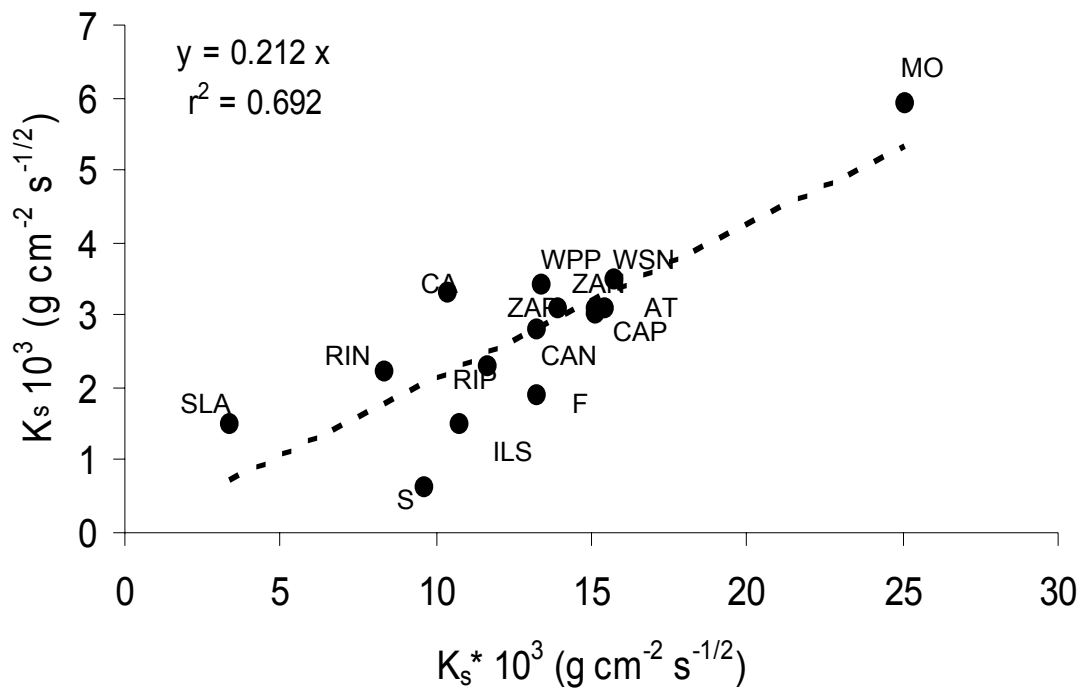
Figure 6. Correlation between the experimental (K_s) and the predicted (K_s*) values of capillarity coefficient.
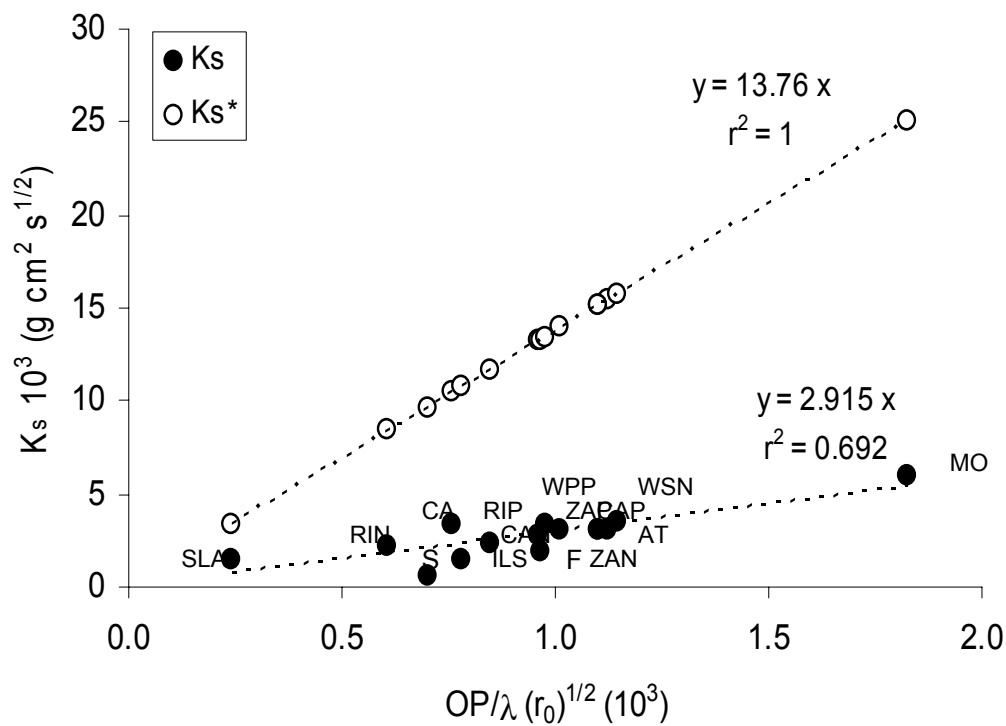
Figure 7. Correlation between the capillary coefficients (experimental and predicted ones) and the term $OP/\lambda \, (r_0)^{1/2}$.
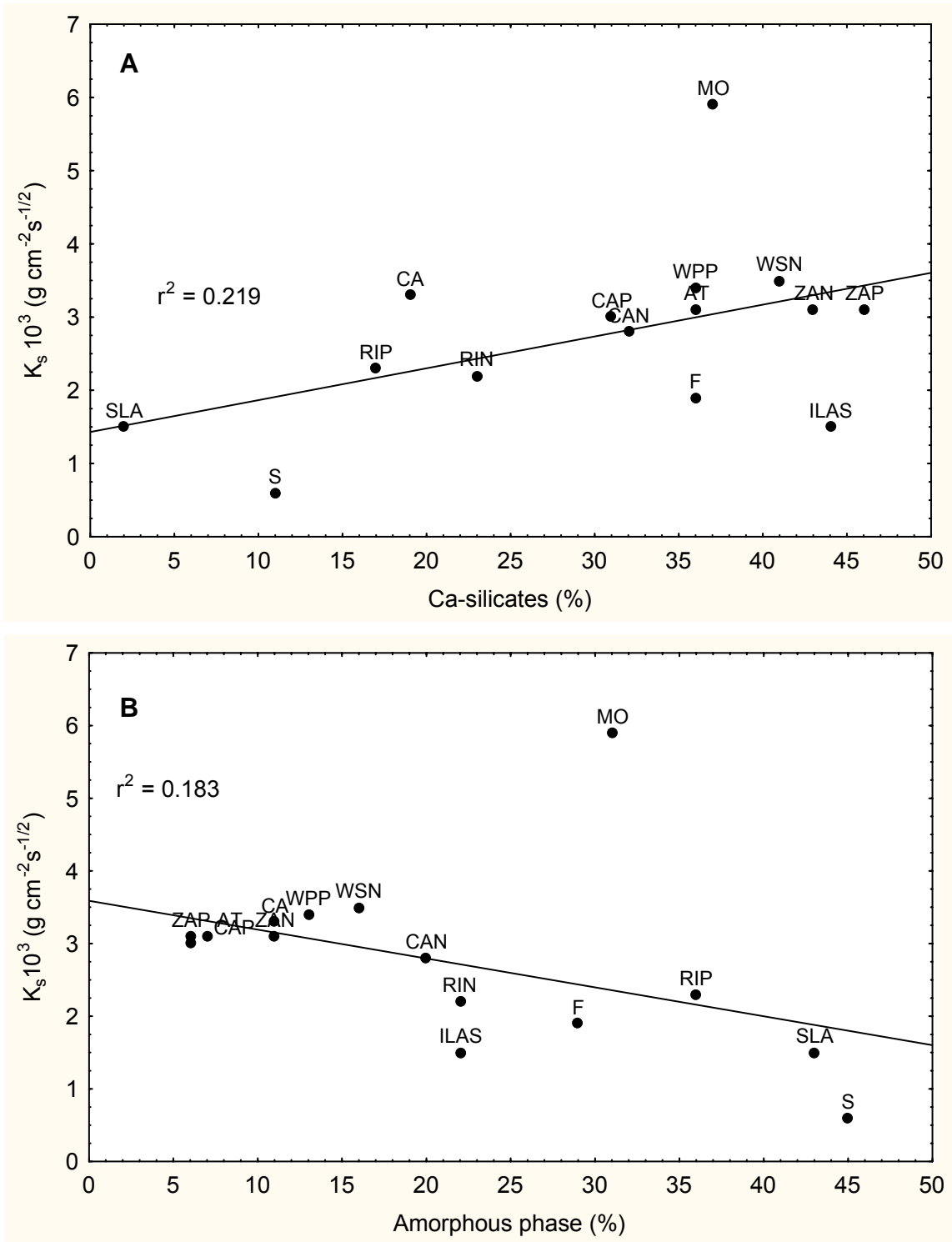
Figure 8. Experimental capillary coefficient K_s vs. the amount of (A) Ca-silicates and (B) amorphous phase of clay bricks.
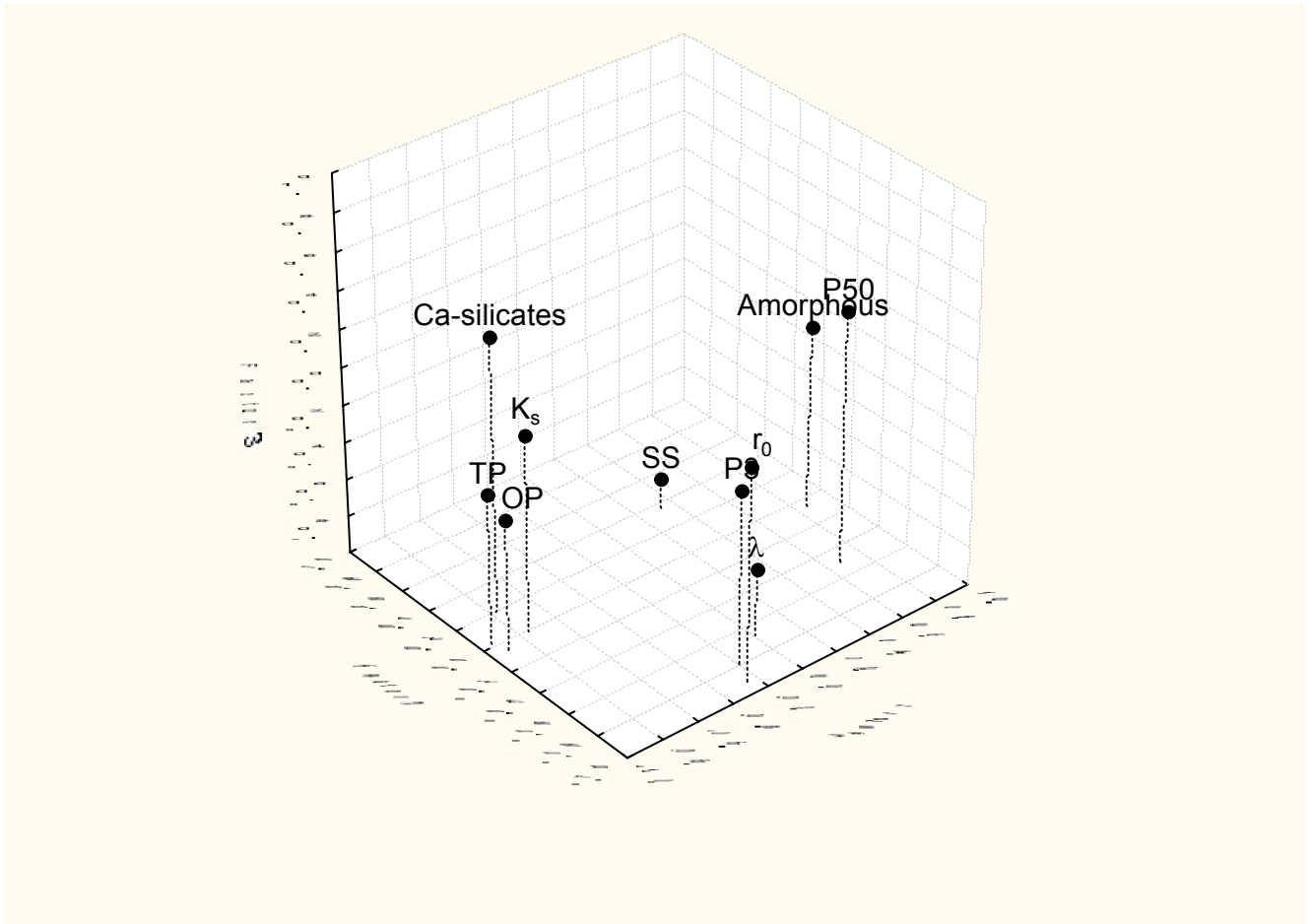
Figure 9. Principal components analysis: factors extracted.
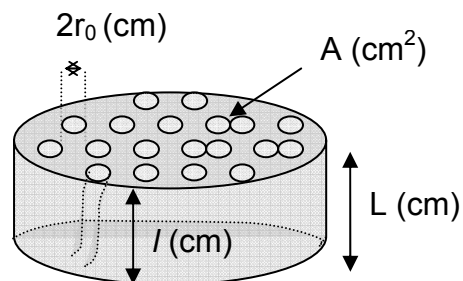
Figure 10. Schematic representation of a cylindrical brick